Eur Biophys J (1987) 14: 131–138

European Biophysics Journal


# Patch clamp characterization of sodium channels expressed from rat brain cDNA

**W. Stühmer [1] *, C. Methfessel [1], B. Sakmann [1], M. Noda [2], and S. Numa [2]**

[1] Max-Planck-Institut für biophysikalische Chemie, D-3400 Göttingen, Federal Republic of Germany,
[2] Departments of Medical Chemistry and Molecular Genetics, Kyoto University Faculty of Medicine, Kyoto, 606 Japan

Received July 15, 1986/Accepted October 2, 1986

**Abstract.** Sodium currents, $I_{Na}$, were recorded from *Xenopus laevis* oocytes which had been injected with mRNA synthesized by *in vitro* transcription of the rat brain sodium channel II cDNA (Noda et al. 1986a, b). Patch pipettes were used to apply depolarizing voltage steps and to record macroscopic sodium currents of between 50 and 750 pA from cell-attached patches of the oocyte membrane. With a combination of whole-cell and patch clamp recording, the properties of the implanted sodium channels could be studied in detail. They were analyzed according to the model of Hodgkin and Huxley (1952a) assuming three activation gates. The activation of the sodium currents is characterized by an equilibrium potential of $-29$ mV and an apparent gating charge of $8.7\,e_0$. At $-64$ mV half of the sodium currents were inactivated. From single-channel current recordings, an elementary sodium channel conductance of 19 pS and an average open time of 0.43 ms were obtained at $-32$ mV membrane potential and 16 °C. The single-channel and activation properties of rat brain sodium channel II are therefore comparable to those found in peripheral nerve and skeletal muscle, but inactivation occurs at less negative potentials. This could be a specific property of the brain sodium channels and may underlie the maintained inward sodium currents reported in brain neurones (French and Gage 1985).

**Key words:** Rat brain sodium channels, cloned sodium channel cDNA, *Xenopus* oocytes, patch clamp

## Introduction

Sodium channels are voltage-sensitive transmembrane proteins essential for the conduction of nerve impulses. Functional sodium channels are expressed in *Xenopus laevis* oocytes after injection of poly(A)$^+$ RNA extracted from rat brain (Gundersen et al. 1983; Sumikawa et al. 1984; Hirono et al. 1985), and detailed properties of the implanted sodium channels can be determined with single-channel recording from such oocytes (Stühmer et al. 1986; Methfessel et al. 1986). The primary structures of the *Electrophorus* electroplax sodium channel (Noda et al. 1984) and of two distinct sodium channel large polypeptides from rat brain named sodium channels I and II (Noda et al. 1986a) have been deduced from the nucleotide sequences of the cloned complementary DNAs. Specific mRNAs transcribed from the rat brain cDNAs direct the synthesis of functional sodium channels in *Xenopus* oocytes (Noda et al. 1986b). In this paper we present a detailed characterization of brain sodium channel II, expressed from the cDNA, which shows that it closely resembles native sodium channels in rat nerve.

The advantages of studying ion channels in oocytes injected with specific mRNA were demonstrated by recent work on the nicotinic acetylcholine receptor (Sakmann et al. 1985; Mishina et al. 1986) where specific functions have been assigned to individual subunits of the receptor. Similarly, the detailed characterization of implanted sodium channels will provide a reference point for the use of site-directed mutagenesis to assign functional properties to specific regions of the sodium channel protein. The characterization of ion channels from single-channel current recording requires the collection and analysis of large amounts of single-channel data. Important properties of ion channels can be obtained much more rapidly and over a wide range of membrane potentials from whole-cell current recording. However, the whole-cell clamp of *Xenopus* oocytes has a poor time resolution (Noda et al. 1986b; Gundersen et al. 1984; Stühmer et al. 1986; Methfessel et al. 1986). In the present study, the whole-cell

* To whom offprint requests should be sent

potential was held constant with a two-electrode voltage clamp while macroscopic sodium currents were recorded from cell-attached patches of the oocyte membrane using the patch clamp method.

## Materials and methods

Messenger RNA specific for rat brain sodium channel II was prepared by transcription in vitro of the recombinant plasmid pRII-1 cleaved with *Sal*I, using the SP6 transcription system (Green et al. 1983; Melton et al. 1984). The plasmid pRII-1 was constructed by ligating the 854-base-pair (bp) *Eco*RI/*Apa*I fragment and the 2,409-bp *Apa*I/*Bgl*II fragment from the plasmid pSRII-1, the ~3.2 kilobase-pair (kb) *Bgl*II/*Xba*I fragment (including the poly(dA) tract) from the plasmid pSRII-2 and the ~3.0-kb *Xba*I/*Eco*RI fragment from the vector plasmid pSP65 (Noda et al. 1986b); pRII-1 carries the same coding sequence as pRII-2 (Noda et al. 1986b) but a longer 5′-noncoding sequence (including three ATG triplets) than pRII-2. For some experiments, the sodium channel II mRNA was derived from pRII-2 as described previously (Noda et al. 1986b). *Xenopus laevis* oocytes at developmental stage *V* were injected with 50 nl of the mRNA in water solution (0.125 μg/μl) and then incubated at 19 °C in modified Barth's medium (Gurdon 1974) containing 50 μg/ml gentamicin. The enveloping follicle cell layer was removed by collagenase treatment on the second day and electrophysiological experiments were done 5–9 days after mRNA injection. Immediately before the experiments, the vitelline membrane was dissected after osmotic shrinking (Sakmann et al. 1985; Methfessel et al. 1986).

Figure 1A illustrates schematically the method of recording multichannel currents from oocytes. The voltage pipettes $P_v$ contained 3 *M* KCl and had resistances in the range of 4 to 6 *M*Ω. The current injection pipettes $P_I$ were filled with (in m*M*) 500 $K_2SO_4$ and 30 KCl, and their tips were gently broken to give resistances of 200–500 kΩ. The extracellular medium and patch pipette filling solution were normal frog Ringer's solution (in m*M*: 115 NaCl, 2.5 KCl, 1.8 $CaCl_2$, 10 HEPES, pH 7.2). Patch pipettes ($P_M$) were made from thin walled aluminosilicate glass. They had resistances between 1.0 and 2.5 *M*Ω when filled with frog Ringer's solution. Sodium currents were recorded from cell-attached patches with seal resistances greater than 3.5 GΩ (Leonard et al. 1986). The mean membrane capacitance, measured according to the method of Sakmann and Neher (1983) for 6 patches, was 1.5 ± 1.0 pF (mean ± SD). Assuming a specific

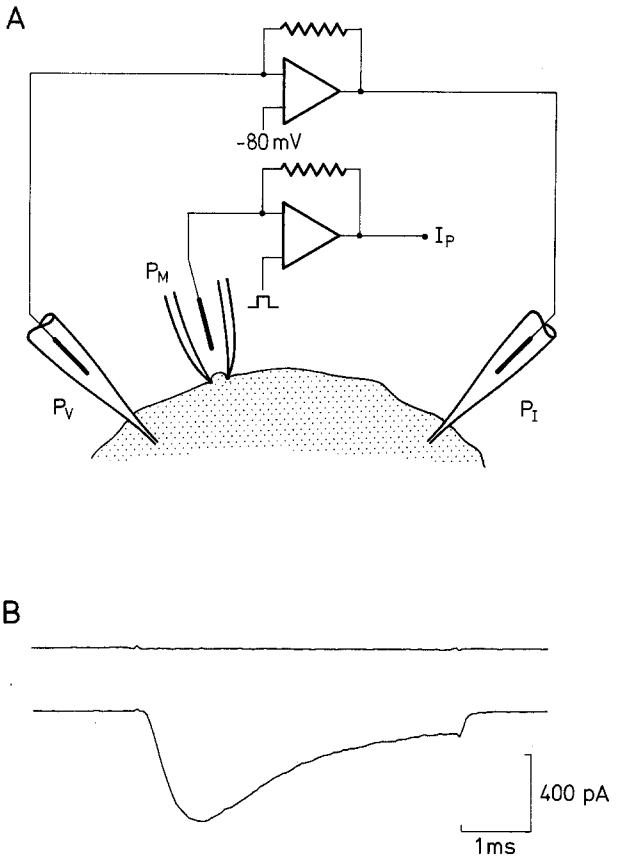


**Fig. 1. A** Schematic representation of the experimental arrangement, $P_v$ is the intracellular voltage recording electrode, $P_I$ is the current injection electrode for the two electrode voltage clamp, and $P_M$ is the patch clamp pipette. **B** A typical current response at −30 mV membrane potential. The *upper trace* shows the *P*/4 transient cancellation signal remaining after analog capacitance compensation and the *lower trace* shows the data record before application of the *P*/4 procedure

membrane capacitance of 1 μF/cm², this corresponds to a mean area of 150 μm², so that the patch areas were between 50 and 400 μm². Due to the high density of sodium channels expressed in the oocyte after injection of the sodium channel II-specific mRNA, such patches contained a large number of sodium channels for recording sodium currents.

The two-electrode voltage clamp was used only to hold the oocyte membrane potential to a constant value of −80 mV. Since fast voltage pulses were not applied to the two-electrode clamp, the speed of the clamp was limited in order to reduce the background noise. Via the patch pipette, the membrane patch was hyperpolarized by 20 mV to a holding potential of −100 mV and depolarizing voltage steps were applied through the patch-clamp amplifier (List EPC-7). Stimulating voltage pulse protocols were generated with a PDP 11/73 laboratory computer. The patch current signals were corrected for capacitive transients with the fast and slow $C_p$ compensa-

tion circuits of the amplifier. The remaining linear components were compensated on-line by the *P*/4 procedure, which involves subtracting current records obtained for smaller depolarizations that do not elicit ionic currents. Figure 1 B illustrates this for a typical current record at −30 mV test potential. The records were digitized and stored by the computer for subsequent analysis.

In order to verify that the membrane potential sensed by the ion channels in the patch was equal to the superposition of the whole-cell holding and the patch pipette command potentials, two tests were carried out. First, sodium currents were recorded from the same patch while the oocyte holding potential was changed between −100 mV to −20 mV and the steady state pipette potential was adjusted to maintain a constant holding potential of −100 mV across the membrane patch. In most cases, the current-voltage relations and the potential-dependent activation and inactivation parameters of the sodium currents did not deviate by more than 4 mV from their average values, showing that voltage control of the patch was satisfactory. Secondly, the whole-cell recording configuration (Hamill et al. 1981) was established by a brief pulse of suction at the end of a patch recording experiment, and the zero-current potential measured with the patch pipette was compared to the command potential imposed by the two-electrode voltage-clamp. In almost all cases the two potentials agreed within 2 mV over a wide range of applied clamp potentials. Poor potential control was found only in some experiments where holding currents greater than 1 μA were required to clamp the whole-cell potential to −80 mV, suggesting a very leaky or damaged oocyte membrane. Such experiments were not included in the analysis presented below.

The sodium channels exhibited a slow inactivation process with time constants in the range of minutes, similar to that described for sodium channels in rat muscle (Simoncini and Stühmer 1986; Ruff et al. 1986) and nerve (Neumcke et al. 1979). Peak sodium currents increased by about 20% when the holding potential was changed from −80 mV to −100 mV. Therefore, newly formed patches were kept for several minutes at the holding potential of −100 mV to allow the full current response to develop before the recording of data commenced.

The density of sodium channels implanted into the oocyte membrane could be estimated roughly from the whole-cell inward currents elicited by depolarizing voltage steps applied to the whole-cell voltage clamp. The very large charging transients were compensated with a three-component RC network, and remaining transients were subtracted with the *P*/4 procedure. Peak sodium current responses ranged from several hundred nA to more than 10 μA, the limit of the voltage clamp amplifier. Assuming an elementary current amplitude of 0.7 pA and an open probability at maximum activation of 0.5 (Sigworth 1980), and estimating the geometric surface area of an oocyte to be $3 \times 10^6\,\mu m^2$, this corresponds to channel densities between 0.5 and at least $10/\mu m^2$. Oocytes with whole-cell current responses greater than 10 μA were selected to obtain large macroscopic sodium currents in cell-attached patches.

### *Single-channel recording*

Because of the high density of sodium channels in the membrane of oocytes injected with the sodium channel II-specific mRNA, single-channel currents could not be resolved in most membrane patches. Therefore, oocytes were injected with a 10-fold diluted mRNA solution to reduce the density of implanted channels. Single-channel sodium currents were recorded with standard aluminosilicate patch pipettes of 1−2 μm tip diameter (Methfessel et al. 1986). Patch pipettes were filled with frog Ringer's solution. The intracellular potential was not clamped, but measured with an intracellular recording electrode. Voltage pulses were applied to the patch pipette and currents were measured with an EPC-7 amplifier. The current signals were recorded on magnetic tape (RACAL 4D) and replayed into the computer for analysis.

## Results

### *Macroscopic sodium currents*

Macroscopic sodium currents were recorded from cell-attached patches of oocytes selected for a large whole-cell current response. The maximal value of the peak sodium current in the patches varied considerably, ranging from 50 pA up to 750 pA. Whereas oocytes injected with poly(A)$^+$ RNA frequently exhibit voltage activated potassium currents and other currents in addition to the sodium current (Gundersen et al. 1984), these were never seen in experiments on oocytes injected with sodium channel-specific mRNA. Also, fast activating sodium currents were never observed in noninjected control oocytes. A slow endogenous voltage-activated sodium current with completely different kinetics has been reported for *Xenopus* oocytes (Baud et al. 1982).

Figure 2A shows a family of sodium currents obtained in response to depolarizing voltage steps of

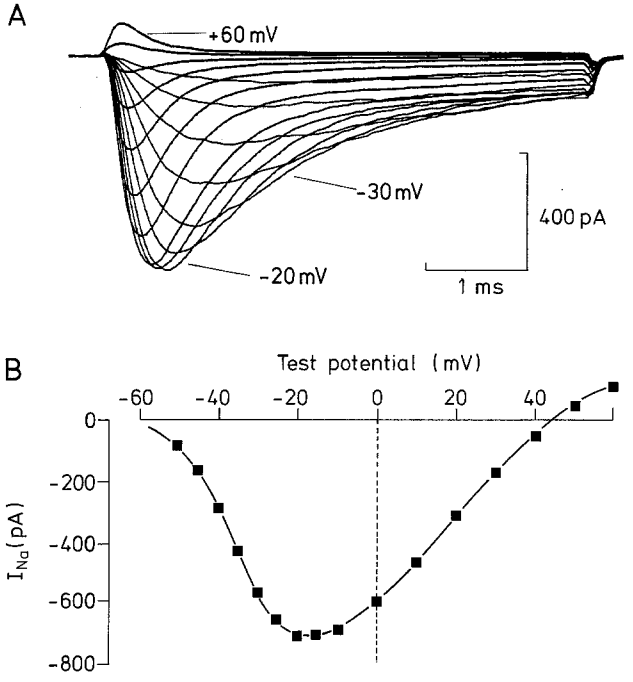


**Fig. 2.** **A** Family of currents elicited in a membrane patch of an oocyte injected with the mRNA specific for rat brain sodium channel II. From a patch holding potential of − 100 mV, depolarizing voltage pulses of 5 ms duration were applied to the patch pipette. The applied test potentials were from − 50 mV to − 10 mV in steps of 5 mV, and continued up to + 60 mV in steps of 10 mV. The current signals were corrected for capacitive transients and leakage as described in the text and filtered through a low pass Bessel filter with 3 dB attenuation at 5 kHz. Each record shown represents the average of 8 consecutive responses. The whole-cell current required to clamp the oocyte to − 80 mV holding potential with the two electrode clamp was 180 nA and the temperature 15 °C. **B** Peak inward current vs. voltage relation for the current records shown in **A**. By interpolation, the reversal potential is $V_{rev} = 45$ mV.

5 ms duration from a holding potential of − 100 mV. Each trace represents the average of 8 records. The peak value of the sodium current for each test potential was obtained from the current records by a third order polynomial fit to the current trace, and is plotted as a function of test pulse potential in Fig. 2 B. In this experiment, the sodium current peak first appeared at − 50 mV and reached a maximum value of 710 pA near − 17 mV. The test potential eliciting the maximal sodium current was fairly constant at − 13.8 ± 4.5 mV (mean ± SD, 46 experiments). The reversal potential of the sodium currents varied between 49 mV and 18 mV and generally decreased during the course of an experiment, probably because of both increasing leakage and accumulation of intracellular sodium.

To study the voltage dependence of the steady-state activation, current responses like those shown in Fig. 2 A were fitted with a mathematical description of sodium current activation kinetics (Hodgkin and Huxley 1952 a). Fits with 2, 3, and 4 independent activation gates were tried and the best fits were obtained by assuming three gates, that is $I = I' m^3 h$. The steady state activation parameter $m_\infty$ was plotted as a function of potential (Fig. 3 A). The relation is characterized by the half-activation potential, $V^m_{1/2}$, at which the open-state probability for each activation gate is one-half, and by the steepness of the potential dependence of activation $a_m$. These parameters were obtained by a least-squares fit (smooth line in Fig. 3 A) to the expression

$$\frac{G_{Na}}{G^{max}_{Na}} = m^3_\infty, \quad m_\infty = \frac{1}{1 + \exp\left(\frac{V^m_{1/2} - V_t}{a_m}\right)}. \tag{1}$$

The average values of the parameters yielding the best fit in two experiments were $V^m_{1/2} = -41$ mV and $a_m = 8.6$ mV. This value of the steepness parameter corresponds to a gating charge of 2.9 $e_0$ per gate. From these values, the equilibrium potential of channel activation is − 29 mV with an effective charge transfer of 8.7 $e_0$.

The voltage dependence of the inactivation parameter $h_\infty$ was measured according to classical analysis (Hodgkin and Huxley 1952 b). Test pulses to a constant value of − 10 mV were applied from various prepulse potentials. With prepulse potentials more positive than − 85 mV, the peak sodium current decreased and it was almost completely inactivated at − 30 mV. The Hodgkin-Huxley inactivation parameter $h_\infty$ was plotted as a function of the prepulse potential (Fig. 3 B) and fitted for each set of data by a nonlinear least-squares procedure according to the equation

$$\frac{I_{Na}}{I^{max}_{Na}} = \frac{1}{1 + \exp\left(\frac{V_{pp} - V^h_{1/2}}{a_h}\right)}. \tag{2}$$

The relation is characterized by the potential $V^h_{1/2}$ at which the sodium current is half inactivated, and by the steepness of the potential dependence $a_h$. In 15 measurements on 9 patches, $V^h_{1/2}$ was − 63.9 ± 5.9 mV (mean ± SD), and $a_h$ was 10.2 ± 1.2 mV. In Fig. 3 B, data reported previously for rat peripheral nerve (Neumcke and Stämpfli 1982) and rat muscle (Almers et al. 1984) are shown (open symbols) for comparison. The value obtained for $a_h$ of rat brain sodium channel II is larger than that reported for other preparations. In the inactivation measurements, there appears to be a small residual current component that inactivates only slowly, if at all, even at large depolarizations. This causes a flattening of the measured inactivation curve and affects the slope determination.

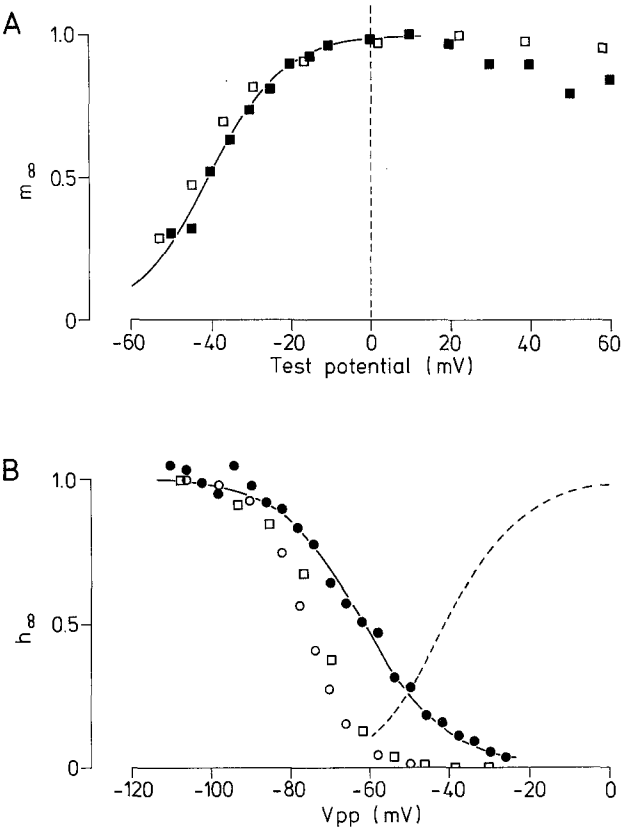


**Fig. 3.** **A** Steady state activation $m_\infty$ of sodium currents as a function of test potential *(filled symbols)*. The *smooth line* represents the best fit to the data as described in the text, with $V^m_{1/2} = -40.5$ mV and $a_m = 9.4$ mV. The *open symbols* represent corresponding values from rat peripheral nerve (Neumcke and Stämpfli 1982). **B** Inactivation of brain sodium currents. Currents were elicited by a test pulse to −10 mV, following conditioning prepulses of 36 ms duration to potentials between −110 mV and −26 mV in steps of 4 mV. The normalized peak inward current responses to the test pulse are plotted as a function of prepulse potential for the rat brain channel II *(filled symbols)*. The *solid line* represents a nonlinear least-squares fit to the data points as described in the text, with $V^h_{1/2} = -62$ mV and $a_h = 10.6$ mV. For comparison, equivalent data from rat peripheral nerve (Neumcke and Stämpfli 1982) are shown as *open squares*, and the *open circles* represent values for rat twitch muscle plotted using $V^h_{1/2} = -76$ mV and $a_h = 5.7$ mV (Almers et al. 1984). The activation relation from Fig. 3A is also shown to indicate the potential range where activation and inactivation overlap *(dashed line)*

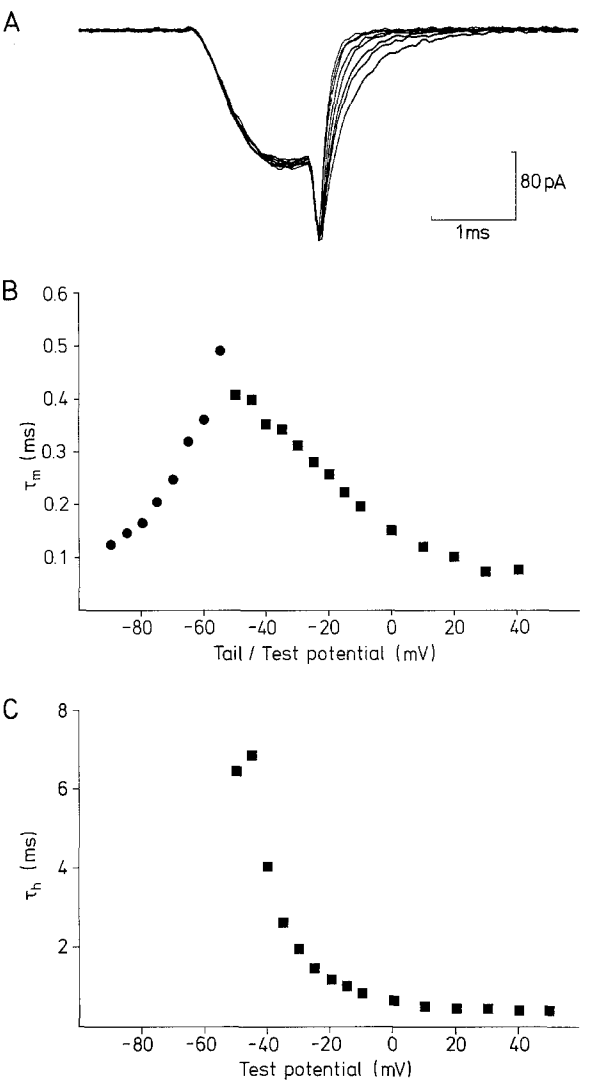


**Fig. 4.** **A** Currents recorded on return to different potentials ("tail currents"). Sodium current was activated by depolarizations to −10 mV, and the patch was repolarized to potentials between −90 mV and −55 mV. Filter setting 10 kHz (−3 dB). Each trace shown is the average of 16 records. Temperature 15 °C. **B** Activation time constant $\tau_m$ as a function of potential. *Circles* represent data obtained from the "tail-" currents shown in **A**, and squares are from Hodgkin and Huxley fits as described in the text. **C** Potential dependent inactivation time constants obtained by fitting the Hodgkin and Huxley model to current traces such as shown in Fig. 2A

*Time constants of activation and inactivation*

The potential dependence of the time constants of activation $\tau_m$ and inactivation $\tau_h$ is shown in Fig. 4. Sodium currents were maximally activated by depolarization to −10 mV, and the patch was then repolarized to "tail" potentials between −90 mV and −55 mV (Fig. 4A). During the repolarization, the activation gates closed with a characteristic time constant. In this way, the potential-dependent kinetics of the activation gates was studied at negative potentials where the steady-state activation is too small for measurable sodium current flow. The tail currents were fitted with single exponentials and the time constants were multiplied by three to give $\tau_m$ according to the Hodgkin-Huxley model. The $\tau_m$ values are plotted in Fig. 4B as filled circles. The activation time constants for potentials more positive than −55 mV (filled squares) were obtained by fitting current records, such as those shown in Fig. 2A, with the equations of Hodgkin and Huxley (1952a). Time constants of inactivation were ob-

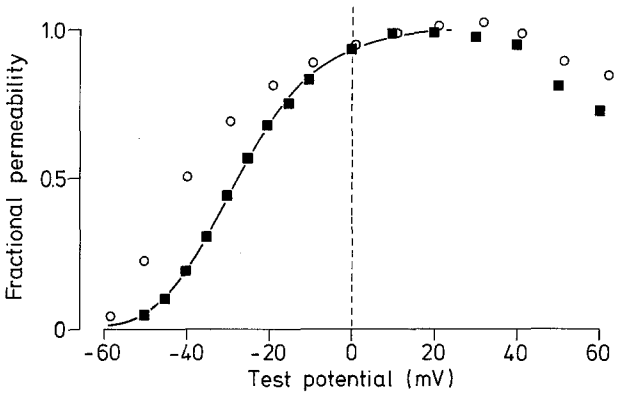


**Fig. 5.** Normalized peak permeabilities (Frankenhaeuser 1960) determined for rat brain sodium channel II *(filled symbols)*. The open symbols give data from rat twitch muscle (Almers et al. 1984) for comparison

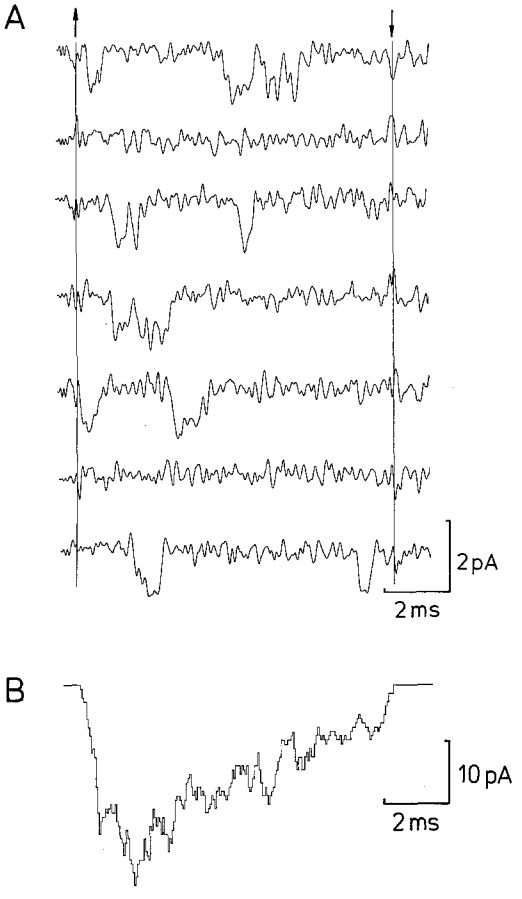


**Fig. 6. A** Currents flowing through single sodium channels. The oocyte resting potential was − 26 mV and the patch was hyperpolarized to − 83 mV membrane potential. Each trace shows the current flowing during a 10 ms depolarization to − 32 mV test potential. To correct for leakage currents, traces showing no channel activity were averaged and subtracted from each record. Current signals were low pass Bessel filtered at 4 kHz (− 3 dB). Temperature was 16 °C. **B** A multichannel current signal reconstructed from 282 idealized single-channel records as described in the text. The time course of the trace is comparable to that of multichannel patch current records at − 35 mV to − 30 mV membrane potential (Fig. 2)

tained from the Hodgkin-Huxley fit together with the activation time constants. Results from a typical experiment are shown in Fig. 4C.

To compare the activation of rat brain sodium channel II with that of sodium channels from rat skeletal muscle, the normalized peak sodium permeability of the brain sodium channels was obtained from the peak inward currents using the constant-field equation (Frankenhaeuser 1960) and plotted in Fig. 5 together with the corresponding data from Almers et al. (1984). It is apparent that in the case of brain sodium channel II the permeability is activated at more positive potentials. As reported for muscle (Almers et al. 1984; Pappone 1980), the permeability values deviate from an asymptote of one at large polarizations and hence the channel does not follow the constant field equation at high positive potentials.

### *Single-channel recordings*

Single-channel current records were obtained from membrane patches showing at most three simultaneous channel openings (see Methods). Figure 6A shows current records elicited from a cell-attached patch by depolarizing voltage steps to a membrane potential of − 32 mV. On depolarization, brief inward current pulses with amplitudes of about 1 pA occur most frequently at the beginning of the depolarizing stimulus but can also be found at later times. Current records were analyzed by the threshold crossing method (Colquhoun and Sigworth 1983). The resulting idealized traces, consisting of rectangular current pulses with the amplitude and duration of the resolved elementary currents, were summed to obtain the record shown in Fig. 6B. The time course of this reconstructed average current closely resembles that of macroscopic sodium currents, with half-maximal rise and decay times that are similar to those found in larger patches with high sodium channel densities at the same potential (Fig. 2).

At any potential, the distribution of single-channel current amplitudes has a single peak and could be fitted with a single Gaussian (Fig. 7A, inset). The mean current $i$ decreased approximately linearly with the potential in the range of − 60 mV to 0 mV, yielding a single-channel conductance of 19 pS at 16 °C (Fig. 7A). An example of the distribution of elementary current durations at a constant potential is shown in Fig. 7B. The mean open time at − 32 mV was in this case 0.43 ms. The properties of rat brain sodium channel II derived from single-channel recording therefore closely resemble those measured for endogenous channels in cultured rat

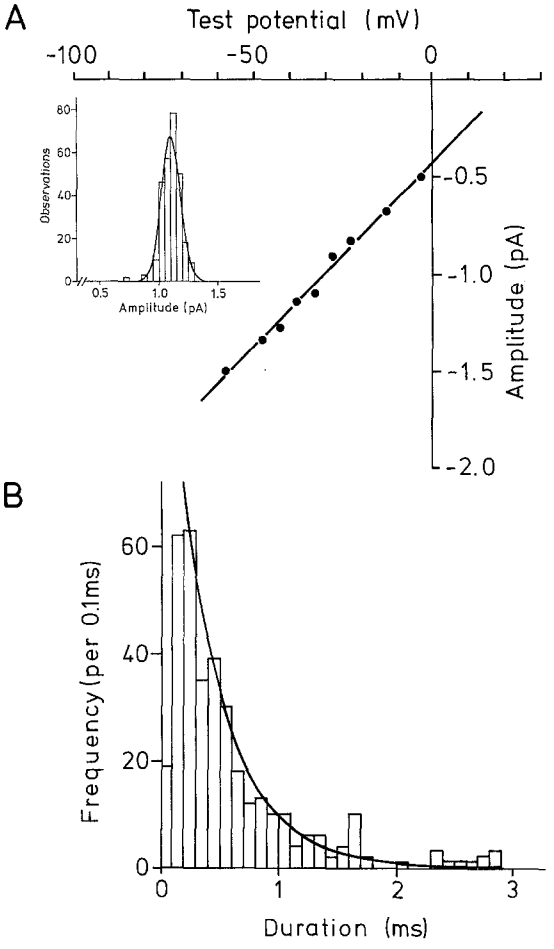


**Fig. 7.** Amplitude and duration of elementary sodium currents. **A** Single-channel current-voltage relation. Each point represents the mean of 20–200 elementary current amplitudes measured at one potential, as shown in the inset for – 32 mV. Minimum duration of 0.1 ms was required for amplitude determination. Data shown are from two experiments with oocyte resting potential of – 26 mV and – 82 mV respectively, with the patch holding potential being – 90 mV in both cases. The straight line fit indicates a slope conductance of 19 pS at 16 °C. **B** Distribution of apparent durations of elementary current pulses recorded at – 32 mV membrane potential. The shortest currents resolved were of 0.1 ms duration. The distribution is fitted with a single exponential decay time constant of 0.43 ms

muscle cells (Sigworth and Neher 1980) and those of sodium channels expressed in oocytes injected with poly(A)$^+$ RNA from rat brain (Stühmer et al. 1986).

## Discussion

It was shown that a combination of the two electrode voltage clamp with the patch clamp technique allows the detailed characterization of rat brain sodium channels expressed in *Xenopus* oocytes. The macroscopic as well as single-channel properties of the sodium channels expressed from the rat brain sodium channel II cDNA (Noda et al. 1986a, b) closely resemble those of other sodium channels described for rat muscle or peripheral nerve. In particular, the steady state activation shows excellent agreement with previous data from rat peripheral nerve (Neumcke and Stämpfli 1982). Only the voltage dependence of steady state inactivation differs significantly in that the half-inactivation potential of the brain sodium channel II is reproducibly shifted by about 10 mV towards less negative potentials. Preliminary experiments on oocytes injected with poly(A)$^+$ RNA extracted from rat muscle (Methfessel et al. 1986) suggest that this difference is not due to the oocyte expression system but may reflect a specific property of brain sodium channels. A consequence of this shift is that the activation and inactivation curves overlap over a wider potential range than in either muscle or peripheral nerve. This is illustrated in Fig. 3B, where the activation curve from Fig. 3A is shown together with the inactivation data. This greater overlap of the steady state activation and inactivation curves in the voltage region between – 60 mV and – 40 mV is expected to produce a slowly inactivating sodium inward current at potentials near the threshold of action potential firing. A persistent inward sodium current in this potential range has been reported in hippocampal neurones (French and Gage 1985) where it is thought to aid the repetitive firing of action potentials.

*Acknowledgements.* We thank Dr. F. Conti, Dr. E. Neher and Dr. F. Sigworth for helpful comments on the manuscript.

## References

Almers W, Roberts WM, Ruff RL (1984) Voltage clamp of rat and human skeletal muscle: measurements with an improved loose-patch technique. J Physiol 347: 751–768

Baud C, Kado RT, Marcher K (1982) Sodium channels induced by depolarization of the *Xenopus laevis* oocyte. Proc Natl Acad Sci USA 79: 3188–3192

Colquhoun D, Sigworth FJ (1983) Fitting and statistical analysis of single-channel records. In: Sakmann B, Neher E (eds) Single-channel recording. Plenum Press, New York, pp 191–263

Frankenhaeuser B (1960) Quantitative description of sodium currents in myelinated nerve fibres of *Xenopus laevis*. J Physiol 151: 491–501

French CR, Gage PW (1985) A threshold sodium current in pyramidal cells in rat hippocampus. Neurosci Lett 56: 289–293

Green MR, Maniatis T, Melton DA (1983) Human β-globin pre-mRNA synthesized *in vitro* is accurately spliced in *Xenopus* oocyte nuclei. Cell 32: 681–694

Gundersen CB, Miledi R, Parker I (1983) Voltage-operated channels induced by foreign messenger RNA in *Xenopus* oocytes. Proc R Soc London B 220: 131–140

Gundersen CB, Miledi R, Parker I (1984) Messenger RNA from human brain induces drug- and voltage-operated channels in *Xenopus* oocytes. Nature 308: 421–424

Gurdon JB (1974) The control of gene expression in animal development. Clarendon Press, Oxford

Hamill OP, Marty A, Neher E, Sakmann B, Sigworth FJ (1981) Improved patch clamp techniques for high-resolution current recording from cells and cell-free membrane patches. Pflügers Arch 391:85–100

Hirono C, Yamagishi S, Ohara R, Hisanaga Y, Nakayama T, Sugiyama H (1985) Characterization of mRNA responsible for induction of functional sodium channels in *Xenopus* oocytes. Brain Res 359:57–64

Hodgkin AL, Huxley AF (1952a) A quantitative description of membrane current and its application to conduction and excitation in nerve. J Physiol 117:500–544

Hodgkin AL, Huxley AF (1952b) The dual effect of membrane potential on sodium conductance in the giant axon of *Loligo*. J Physiol 116:497–506

Leonard J, Snutch T, Lubbert H, Davidson N, Lester HA (1986) Macroscopic Na currents with gigaohm seals on mRNA-injected *Xenopus* oocytes. Biophys J 49:386a

Melton DA, Krieg PA, Rebagliati MR, Maniatis T, Sinn K, Green MR (1984) Efficient in vitro synthesis of biologically active RNA and RNA hybridization probes from plasmids containing a bacteriophage SP6 promoter. Nucleic Acids Res 12:7035–7056

Methfessel C, Witzemann V, Takahashi T, Mishina M, Numa S, Sakmann B (1986) Patch clamp measurements on *Xenopus laevis* oocytes: Currents through endogenous channels and implanted acetylcholine receptor and sodium channels. Pflügers Arch (in press)

Mishina M, Takai T, Imoto K, Noda M, Takahashi T, Numa S, Methfessel C, Sakmann B (1986) Molecular distinction between fetal and adult forms of muscle acetylcholine receptor. Nature 321:406–411

Neumcke B, Stämpfli R (1982) Sodium currents and sodium-current fluctuations in rat myelinated nerve fibres. J Physiol 329:163–384

Neumcke B, Schwarz W, Stämpfli R (1979) Slow actions of hyperpolarization on sodium channels in the membrane of myelinated nerve. Biochim Biophys Acta 558:113–118

Noda M, Shimizu S, Tanabe T, Takai T, Kayano T, Ikeda T, Takahashi H, Nakayama H, Kanaoka Y, Minamino N, Kangawa K, Matsuo H, Raftery MA, Hirose T, Inayama S, Hayashida H, Miyata T, Numa S (1984) Primary structure of *Electrophorus electricus* sodium channel deduced from cDNA sequence. Nature 312:121–127

Noda M, Ikeda T, Kayano T, Suzuki H, Takeshima H, Kurasaki M, Takahashi H, Numa S (1986a) Existence of distinct sodium channel messenger RNAs in rat brain. Nature 320:188–192

Noda M, Ikeda T, Suzuki H, Takeshima H, Takahashi T, Kuno M, Numa S (1986b) Expression of functional sodium channels from cloned cDNA. Nature 322:826–828

Pappone PA (1980) Voltage-clamp experiments in normal and denervated mammalian skeletal muscle fibres. J Physiol 306:377–410

Ruff RL, Simoncini L, Stühmer W (1987) Comparison between slow sodium channel inactivation in rat slow and fast twitch muscle. J Physiol 383:339–348

Sakmann B, Neher E (1983) Geometric parameters of pipettes and membrane patches. In: Sakmann B, Neher E (eds) Single-channel recording. Plenum Press, New York, pp 37–51

Sakmann B, Methfessel C, Mishina M, Takahashi T, Takai T, Kurasaki M, Fukuda K, Numa S (1985) Role of acetylcholine receptor subunits in gating of the channel. Nature 318:538–543

Sigworth FJ (1980) The variance of sodium current fluctuations at the node of Ranvier. J Physiol 307:97–129

Sigworth FJ, Neher E (1980) Single $Na^+$ channel currents observed in cultured rat muscle cells. Nature 287:447–449

Simoncini L, Stühmer W (1987) Slow sodium inactivation in rat fast twitch muscle. J Physiol 383:327–337

Stühmer W, Methfessel C, Witzemann V, Sakmann B (1986) Rat brain sodium channels recorded from *Xenopus* oocytes. In: Lüttgau HC (ed) Membrane control of cellular activity, vol 33. G Fischer, Stuttgart, pp 155–159

Sumikawa K, Parker I, Miledi R (1984) Partial purification and functional expression of brain mRNAs coding for neurotransmitter receptors and voltage operated channels. Proc Natl Acad Sci USA 81:7994–7998